



Benzothiazole appended lower rim 1,3-di-amido-derivative of calix[4]arene: Synthesis, structure, receptor properties towards Cu²⁺, iodide recognition and computational modeling

Roymon Joseph, Jugun Prakash Chinta, Chebrolu P. Rao *

Bioinorganic Laboratory, Department of Chemistry, Indian Institute of Technology Bombay, Powai, Mumbai 400 076, India

ARTICLE INFO

Article history:

Received 29 December 2009
Received in revised form 30 March 2010
Accepted 6 April 2010
Available online 18 April 2010

Dedicated to Animesh Chakravorty

Keywords:

1,3-Di-benzothiazole-amido-derivative of calix[4]arene (L)
Selective recognition of Cu²⁺
Fluorescence quenching
S₂O₂ binding core of L
DFT computations
ESI-MS

ABSTRACT

A new molecular fluorescent sensor (L) for Cu²⁺ has been synthesized by derivatizing the lower rim of calix[4]arene with benzothiazole moiety, through amide linkage to result in 1,3-di-derivative. The receptor molecule, L exhibited fluorescence quenching towards Cu²⁺ among eleven divalent ions, viz., Mn²⁺, Fe²⁺, Co²⁺, Ni²⁺, Cu²⁺, Zn²⁺, Cd²⁺, Hg²⁺, Ca²⁺, Mg²⁺ and Pb²⁺, studied. The 1:1 stoichiometry of the complex formed between L and Cu²⁺ has been demonstrated by electronic absorption and ESI-MS. The role of calix[4]arene for the selective sensing of Cu²⁺ has been established by comparing the data with that obtained for an appropriate control molecule. The minimum concentration at which L can detect Cu²⁺ has been found to be 403 ppb. The computations carried out at DFT level have provided the coordination and structural features of the Cu²⁺ complex of L as species of recognition. The Cu²⁺ complex thus formed recognizes iodide by bringing change in the color, among the 14 anions studied.

© 2010 Elsevier B.V. All rights reserved.

1. Introduction

Copper is one of the top three biologically essential elements [1] involved in exhibiting a variety of oxidative functions including electron transfer [2–5], while iodide is involved only in the thyroid function [6,7]. Insufficiency or overload of this element results in various neurodegenerative disorders [8,9] and the insufficiency of iodine results in goiter [10,11]. This necessitates the development of receptors for selective recognition of Cu²⁺ and I[−]. Calix[4]arenes [12] are important class of macrocyclic compounds possessing both hydrophilic and hydrophobic regions and hence are suited for receiving cations and anions selectively. Calix[4]arene derivatives can be synthesized easily by introducing moieties having different functional groups that can bind to metal ions through nitrogen, sulfur or oxygen ligating centers [13–19]. Calix[4]arene based receptors for the selective recognition of Cu²⁺ as well as I[−] are rather limited in the literature [20–28]. This includes, the report of a 1,3-di-derivative of calix[4]arene bearing anthracene–isoxazolymethyl at the lower rim by Chung et al. [20], which revealed chemosensor properties towards Cu²⁺ by fluorescence quenching. Other literature reports for Cu²⁺ sensing by calix[4]arene derivatives includes quinoline [21] or 5-nitro salicylaldehyde [22] group connected to

the upper rim of calix[4]arene through an imine moiety. Among the lower rim functionalized derivatives, 3-alkoxy-2-naphthoic acid [23] and coumarin [24] appended calix[4]arenes are a few examples for Cu²⁺ sensing. Our research group recently demonstrated the selective recognition of some biologically relevant cations, viz., Zn²⁺ [29,30], Zn²⁺ and Ni²⁺ [31] and Cu²⁺ [32], as well as environmentally relevant heavy metal ion, viz., Hg²⁺ [33] in addition to an anion, viz., iodide [34] by 1,3-di-derivatives of calix[4]arene. In this paper we report the synthesis, characterization, and cation and anion binding properties of a new 1,3-di-derivative of calix[4]arene connected to a benzothiazole moiety through amide linkage (L) as a fluorescent sensor for Cu²⁺ and the corresponding complex as absorption sensor for I[−]. Fluorescence, absorption and ESI-MS techniques have been used for studying the binding properties. The studies were compared with appropriate control molecules. The coordination and structural features of the Cu²⁺ complex of L has been demonstrated by computational calculations at DFT level.

2. Experimental

2.1. General

All the metal salts used in the titrations were as their perchlorate salts (Caution: perchlorate salts may explode under certain

* Corresponding author. Fax: +91 22 2572 3480.
E-mail address: cp Rao@iitb.ac.in (C.P. Rao).

conditions) with a formula, $M(\text{ClO}_4)_2 \cdot x\text{H}_2\text{O}$ and these were procured from Sigma Aldrich Chemical Co., U.S.A. Sodium salts of anions, viz.; F^- , Cl^- , Br^- , I^- , ClO_4^- , SCN^- , AcO^- , SO_4^{2-} , CO_3^{2-} , NO_3^- , HSO_3^- , HPO_4^{2-} , NO_2^- and N_3^- have been used for the titrations and were procured from local sources. All the solvents used were of analytical grade and were purified and dried by routine procedures immediately before use. ^1H and ^{13}C NMR spectra were recorded on a Varian Mercury NMR spectrometer working at 400 MHz. The mass spectra were recorded on Varian Inc, U.S.A. spectrometer using electrospray ionization method. Steady state fluorescence spectra were measured on Perkin-Elmer LS55. The absorption spectra were measured on Shimadzu UV2101 PC. The elemental analysis was performed on ThermoQuest microanalysis. FTIR spectra were measured on Perkin-Elmer spectrometer using KBr pellets. Single crystal X-ray diffraction data were collected on an OXFORD DIFFRACTION XCALIBUR-S CCD system by ω - 2θ scan mode and the absorption corrections were applied by using multi-scan method. The structure was solved by direct methods and refined by full-matrix least squares against F^2 using SHELXL-97. Non-hydrogen atoms were refined with anisotropic thermal parameters. All the hydrogen atoms were geometrically fixed and allowed to refine using a riding model.

2.2. Solutions for fluorescence and absorption studies

Fluorescence emission spectra were measured by exciting the solutions in acetonitrile at 300 nm and the emission spectra were recorded in 320–500 nm range. The fluorescence studies performed in CH_3CN solution uses always a 50 μl solution of **L**. All the measurements were made in 1 cm quartz cell and maintained a final **L** concentration of 10 μM . During the titration, the concentration of metal perchlorate was varied accordingly in order to result in requisite mole ratios of metal ion to **L** and the total volume of the solution was maintained constant at 3 mL in each case by adding CH_3CN . All the absorption studies were carried out in Shimadzu UV-2101 PC by using 10 μM solution of **L**. Same procedure has been followed for the titration of the reference molecule, **L**₁ with metal ions.

2.3. Synthesis and characterization of receptor and control molecule

The receptor molecule **L** has been synthesized by four known steps [35–38] starting from *p*-*tert*-butylcalix[4]arene as given in Scheme 1 (SI O1). All the precursor molecules and the receptor molecule, **L** have been well characterized by NMR, ESI MS, IR and elemental analysis. The receptor molecule, **L** exists in cone conformation as confirmed by both NMR spectra and single crystal XRD

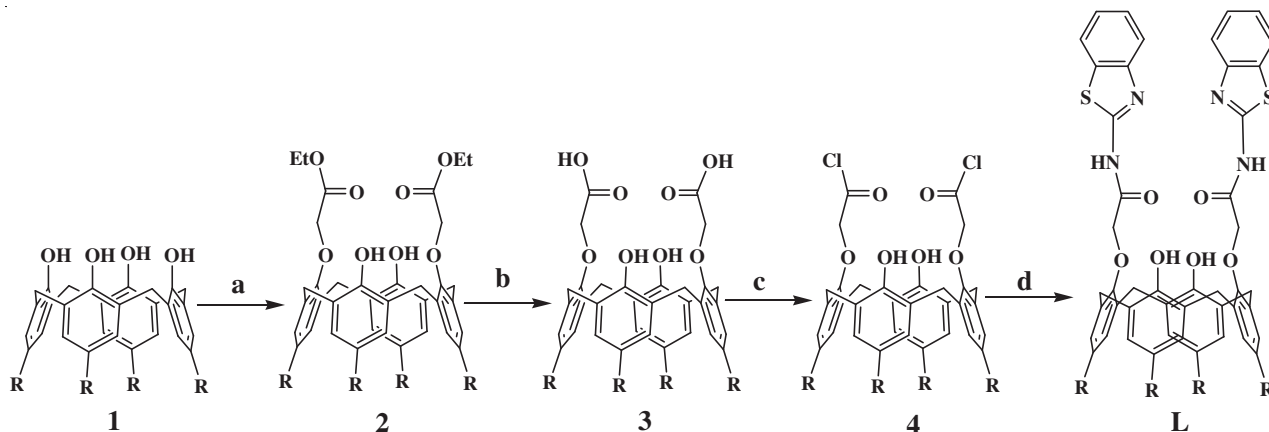
studies. The reference molecule **L**₁ has been synthesized as shown in Scheme 2 (SI O1) and was well characterized.

2.4. Synthesis and characterization of 5,11,17,23-tetra-*tert*-butyl-25,27-bis((2-benzothiazole)carbonylmethoxy)-26,28-dihydroxycalix[4]arene (**L**)

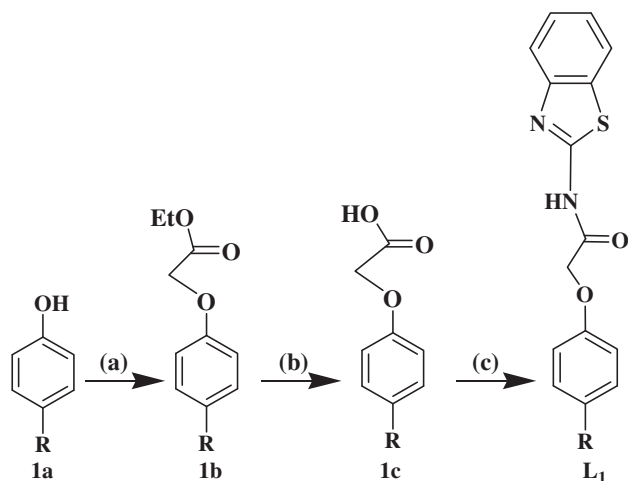
A suspension of 2-aminobenzothiazole (0.89 g, 5.9 mmol) and Et_3N (1.5 mL, 10.78 mmol) was stirred in dry THF (50 mL) under argon atmosphere. Diacid chloride, **4** (2.16 g, 2.70 mmol) in dry THF (80 mL) was added drop wise to this reaction mixture. Immediately, a yellowish precipitate was formed and stirring was continued for 48 h at room temperature. After filtering, the filtrate was concentrated to dryness. A yellow solid was obtained which was extracted with CHCl_3 , washed with water and then with brine and the organic layer was dried over anhydrous MgSO_4 . Filtrate was concentrated to dryness and re-crystallised from $\text{EtOH}/\text{CHCl}_3$ to get **L** as white solid. Yield (50%, 1.42 g) $\text{C}_{62}\text{H}_{68}\text{N}_4\text{S}_2\text{O}_6$ (1029.35). Anal. Calc. for $\text{C}_{62}\text{H}_{68}\text{N}_4\text{S}_2\text{O}_6$. $\text{C}_2\text{H}_5\text{OH}$: C, 71.48; H, 6.93; N, 5.22; S, 5.96. Found C 71.57, H 6.61, N 5.68, S 5.65%. FTIR: (KBr, cm^{-1}): 1702 ($\nu_{\text{C=O}}$), 3424 (ν_{OH}). ^1H NMR: (CDCl_3 , δ ppm): 1.10 (s, 18H, $\text{C}(\text{CH}_3)_3$), 1.19 (s, 18H, $\text{C}(\text{CH}_3)_3$), 3.51 (d, 4H, Ar- CH_2 -Ar, $J = 13.14$ Hz), 4.23 (d, 4H, Ar- CH_2 -Ar, $J = 13.14$ Hz), 4.81 (s, 4H, - CH_2CONH -), 7.04 (s, 4H, Ar-H), 7.06 (s, 4H, Ar-H), 7.20 (t, 2H, benzothiazole **H**, $J = 7.33$ Hz), 7.37 (t, 2H, benzothiazole, $J = 7.03$ Hz), 7.53 (d, 2H, benzothiazole **H**, $J = 7.94$ Hz), 7.66 (d, 2H, benzothiazole, $J = 7.94$ Hz), 8.72 (s, 2H, -OH), 12.29 (s, 2H, -NH). ^{13}C NMR: (CDCl_3 , 100 MHz δ ppm): 31.2, 31.7 ($\text{C}(\text{CH}_3)_3$), 32.7 (Ar- CH_2 -Ar), 34.0, 34.4 ($\text{C}(\text{CH}_3)_3$), 74.3 (OCH_2CO), 120.8, 121.6, 123.7, 125.8, 125.9, 126.4, 126.6, 132.3, 132.6, 143.2, 148.7, 149, 149.8, 156.6 (benzothiazole and calix-Ar-C), 166.5 (C=O). m/z (ES-MS) 1029.45 ($[\text{M}]^+$ 100%), 1030.45 ($[\text{M}+\text{H}]^+$ 25%). Single crystals of **L** were obtained by slow evaporation of the solvent mixture ($\text{EtOH}/\text{CHCl}_3$) at room temperature.

2.5. Synthesis and characterization of 2-(4-*tert*-butylphenoxy)-*N*-(benzothiazol-2-yl)acetamide (**L**₁)

To a solution of **1c** (0.5 g, 2.40 mmol) in CH_2Cl_2 (85 mL) was added Et_3N (1.40 mL, 9.59 mmol), 1-ethyl-(3-dimethylaminopropyl)-3-carbodiimide hydrochloride (EDCI. HCl) (0.69 g, 3.60 mmol) and a catalytic amount of 1-hydroxybenzotriazole (HOBT) and stirred the solution at 0 °C for 30 min under N_2 atmosphere. 2-Aminobenzothiazole (0.54 g, 3.60 mmol) was added to this reaction mixture and stirred at room temperature overnight. The resulting mixture was washed with water followed by saturated NaHCO_3 and brine. The product has been purified by silica gel column



Scheme 1. Synthesis of lower rim calix[4]arene-1,3-di-amido-benzothiazole derivative, **L**: (a) ethyl bromoacetate/ K_2CO_3 /acetone; (b) $\text{NaOH}/\text{C}_2\text{H}_5\text{OH}$, reflux; (c) SOCl_2 /benzene, reflux; (d) 2-aminobenzothiazole/ $\text{Et}_3\text{N}/\text{THF}$. R = *tert*-butyl.



Scheme 2. Synthesis of L_1 : (a) ethyl bromoacetate/ K_2CO_3 /acetone; (b) KOH/ C_2H_5OH /water, reflux; and (c) 2-aminobenzothiazole/ Et_3N /EDCI. HCl/HOBT/ CH_2Cl_2 . R = *tert*-butyl.

chromatography using chloroform–methanol (9.5:0.5) as eluent to give white solid. Yield (0.51 g, 62%). $C_{19}H_{20}N_2SO_2$ (340.44). *Anal.* Calc. for $C_{19}H_{20}N_2SO_2$: C, 66.82; H, 5.98; N, 8.52; S, 9.36. Found. C 67.03, H 5.92, N 8.23, S 9.42%. FTIR: (KBr, cm^{-1}): 1686 ($\nu_{C=O}$). 1H NMR: ($CDCl_3$, δ ppm): 1.31 (s, 9H, $C(CH_3)_3$), 4.73 (s, 2H, OCH_2), 6.90 (d, 2H, Ar-H, $J = 8.55$ Hz), 7.32–7.38 (m, 3H, Ar-H & Benz-H), 7.46 (t, 1H, Benz-H, $J = 8.25$ Hz), 7.80–7.85 (m, 2H, Benz-H), 9.98 (s, 1H, CONH). ^{13}C NMR: ($CDCl_3$, 100 MHz δ ppm): 31.5 ($C(CH_3)_3$), 34.3 ($C(CH_3)_3$), 67.0 (OCH_2CO), 114.2, 121.3, 121.5, 124.3, 126.4, 126.7, 132.3, 145.5, 148.3, 154.5, 156.9 (Benz and Phenyl Ar-C), 167.3 ($C=O$). m/z (ES-MS) 341.12 ($[M+H]^+$ 25%).

3. Results and discussions

3.1. Crystal structure of L

Slow evaporation of a solution mixture of $CHCl_3$ and ethanol containing **L** resulted in good quality single crystals suitable for X-ray diffraction studies and the corresponding crystallographic data fits well with triclinic system with space group $P\bar{1}$ (SI 02) and the corresponding crystallographic parameters were given in Table 1. The asymmetric unit cell possesses one molecule of **L**, two molecules of $CHCl_3$ and one molecule of C_2H_5OH . The intramolecular hydrogen bonding present at the lower rim of calix[4]arene fixes the ligand **L** in cone conformation (Fig. 1a). The inter rim hydrogen bonds exhibited donor...acceptor distances of 2.674(2) and 2.672(2) Å respectively between the unsubstituted phenolic –OH and oxygen of the substituted arm. The amide CO of both the arms point outside the calix[4]arene cavity. The distance between the CO and S was observed to be 2.705(3) and 2.731(3) Å in both the arms suggesting an almost symmetric distribution of these moieties with respect to the calix[4]arene frame. Further, the amide NH present in each of the arms make a hydrogen bond with the phenolic-OH located at lower rim with N...O distances of 2.967(3) and 2.874(4) Å. The ethanol molecule sits inside the arene cavity without extending any interactions. In the lattice, the molecules are arranged in columns and the chloroform molecules present between these columns do not extend any interactions with **L** (Fig. 1b).

3.2. Fluorescence titration studies

The binding ability of **L** towards M^{2+} has been studied by fluorescence spectroscopy in acetonitrile at 10 μM by exciting **L** at 300 nm

Table 1
Crystallographic parameters for the structure determination and refinement.

L	
Empirical formula	$C_{62}H_{68}N_4O_6S_2 \cdot 2CHCl_3 \cdot C_2H_5OH$
Molecular weight	1314.15
T (K)	293
Crystal system	Triclinic
Space group	$P\bar{1}$ (no. 2)
a (Å)	14.575 (3)
b (Å)	15.184 (3)
c (Å)	16.347 (3)
α (°)	79.82 (3)
β (°)	74.823 (3)
γ (°)	75.19 (3)
V (Å ³)	3352.2 (1)
Z	2
Absorption coefficient (mm^{-1})	0.373
D_{calc} . ($g\ cm^{-3}$)	1.302
Reflections collected	52 819
Unique reflections	22 167
R_{int}	0.035
Reflections used	22 167
Parameters	761
Final R	0.0812
wR_2	0.2602

and recording the emission spectra in the range 320–500 nm wherein the emission maximum was observed ~ 355 nm. The metal ions used in the recognition studies include, Mn^{2+} , Fe^{2+} , Co^{2+} , Ni^{2+} , Cu^{2+} , Zn^{2+} , Cd^{2+} , Hg^{2+} , Pb^{2+} , Mg^{2+} and Ca^{2+} . The fluorescence intensity gradually diminishes as a function of the addition of Cu^{2+} and a saturation in its quenching is observed at $[Cu^{2+}]/[L]$ mole ratio greater than 10 suggesting that the binding is an equilibrium driven reaction (Fig. 2a). All the other M^{2+} ions have not shown any appreciable change in the fluorescence intensity indicating their non-interactive nature towards **L** (Fig. 2b). The fluorescence quenching fold observed in case of **L** with Cu^{2+} is 8 ± 0.6 and yields a K_a of $18893 \pm 1200\ M^{-1}$ based on Benesi–Hildebrand equation. The minimum concentration at which **L** can detect Cu^{2+} has been found to be 403 ppb as measured based on dilution experiment carried out by keeping Cu^{2+} to **L** ratio at 1:1 (SI 03).

The role of calix[4]arene platform in the selective recognition of Cu^{2+} has been examined by comparing the fluorescence results of **L** with a single strand derivative (L_1 , Scheme 2) having *p-tert*-butylphenoxy moiety instead of calix[4]arene platform, with M^{2+} ions, viz., Mn^{2+} , Fe^{2+} , Co^{2+} , Ni^{2+} , Cu^{2+} , Zn^{2+} , Cd^{2+} , Hg^{2+} , Ca^{2+} , Mg^{2+} and Pb^{2+} . None of the M^{2+} including Cu^{2+} showed appreciable change in the fluorescence intensity during the titration indicating that L_1 is nonselective and hence supports the necessity of calix[4]arene platform for selective recognition of Cu^{2+} (Fig. 3).

3.3. Absorption and ESI-MS titration studies

The binding of **L** with Cu^{2+} has been further demonstrated by absorption spectroscopy wherein the spectrum of **L** exhibits mainly three bands at 300, 288 and 275 nm, respectively (Fig. 4a). The bands at 252 and 300 nm showed increase in absorbance upon Cu^{2+} addition (SI 03). The stoichiometry of the Cu^{2+} and **L** complex has been calculated to be 1:1 based on the Job's plot (Fig. 4b). A more direct evidence for the formation of 1:1 complex has been obtained by ESI mass spectrum when one equivalent of Cu^{2+} was added to a solution of **L** in CH_3CN (SI 04). The ESI-MS spectrum of **L** with Cu^{2+} resulted in a molecular ion peak at m/z of 1091.6 corresponding to a 1:1 species of Cu^{2+} and **L**, and the presence of Cu^{2+} in this species has been shown based on the isotopic peak pattern observed with this peak (Fig. 4c). The 1H NMR

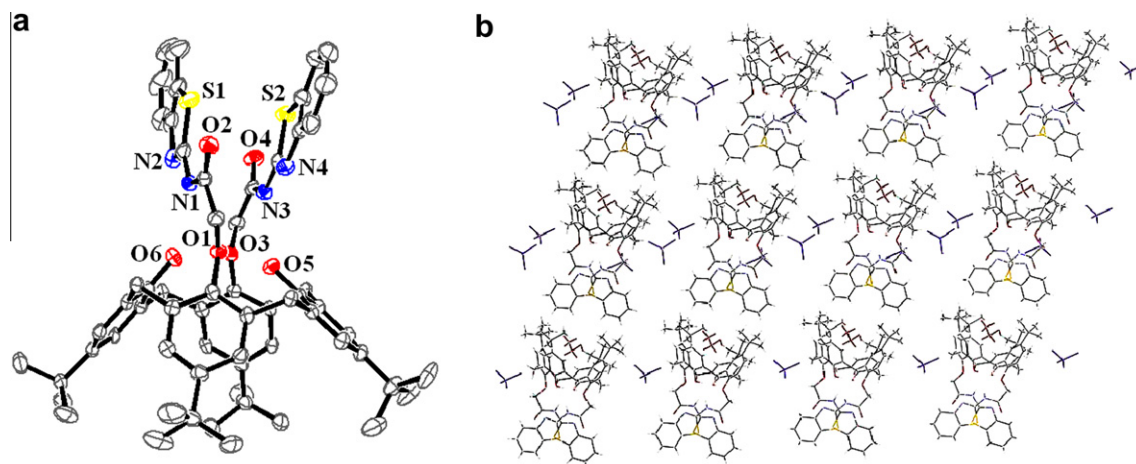


Fig. 1. (a) Single crystal XRD structure of **L** as ORTEP. (b) Lattice structure of **L** inclusive of the solvent molecules.

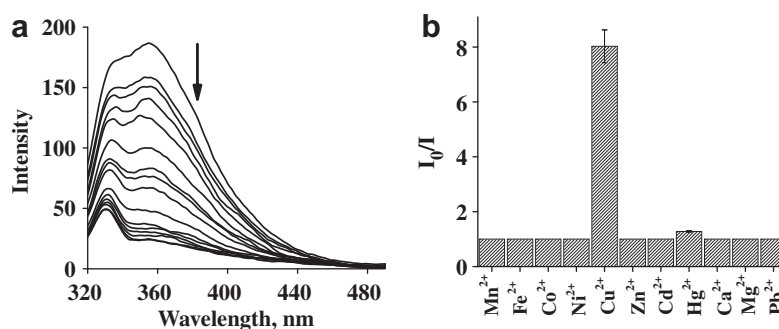


Fig. 2. (a) Fluorescence spectral traces obtained during the titration of **L** with different mole ratios of Cu^{2+} . (b) Histogram representing the changes in the fluorescence response of **L** in presence of different M^{2+} ions.

titration revealed the formation of Cu^{2+} complex of **L** by exhibiting broadened signals owing to the presence of paramagnetic Cu^{2+} .

3.4. Competitive metal ion titrations

In order to explore the practical utility of **L** as an ion-selective fluorescence chemosensor for Cu^{2+} , competitive experiments were carried out in presence of other metal ions by titrating 1:10 equivalents of **L** and Cu^{2+} with different mole ratio of other M^{2+} ions.

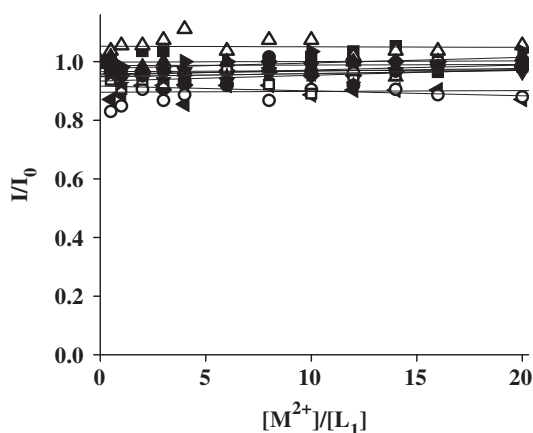


Fig. 3. Plot of relative fluorescence intensity I/I_0 vs. mole ratio of M^{2+} during the titration. The symbols corresponds to \blacksquare = Mn^{2+} ; \triangle = Fe^{2+} ; \blacktriangle = Co^{2+} ; \blacktriangledown = Ni^{2+} ; \blacktriangleleft = Cu^{2+} ; \blacktriangleright = Zn^{2+} ; \blacklozenge = Cd^{2+} ; \circ = Hg^{2+} ; \square = Ca^{2+} ; \bullet = Mg^{2+} and \star = Pb^{2+} .

These titrations resulted in no significant change in the fluorescence intensity suggesting that other M^{2+} ions do not replace Cu^{2+} from the binding site of **L** even after 50 equivalent addition of these ions (Fig. 5), viz., a selective binding for Cu^{2+} . Thus it may be concluded that **L** is a potential Cu^{2+} selective receptor even in the presence of other divalent metal ions.

3.5. Computational studies

In order to establish the coordination and structural features of the species of recognition, computational calculations were carried out using GAUSSIAN 03 package [39]. The crystal structure of **L** has been taken as initial guess and was optimized by replacing each *tert*-butyl group in **L** by hydrogen. Replacement of *tert*-butyl group by hydrogen has been done in order to reduce the computational times without compromising the chemical and conformational features of the derivative. The calculations were performed in a cascade fashion by going through different levels of theories, viz., AM1 \rightarrow HF/STO3G \rightarrow HF/3-21G. The optimization of the complex was carried out by simply placing the Cu^{2+} far above the binding core so that there are no interactions present between **L** and Cu^{2+} in the beginning. The final optimization of the copper complex has been carried out by DFT method using B3LYP/6-31g*. The resultant structure has been further subjected to the interaction with acetonitrile. The optimization carried out in the presence of acetonitrile in B3LYP/6-31g* resulted in a complex where Cu^{2+} exhibit a distorted trigonal bipyramidal geometry wherein each arm of **L** acts as bidentate in filling a total of four coordinations, and the fifth coordination comes from acetonitrile, resulting in a NO_2S_2 binding core (Fig. 6a). Comparison of the crystal structure of **L** with

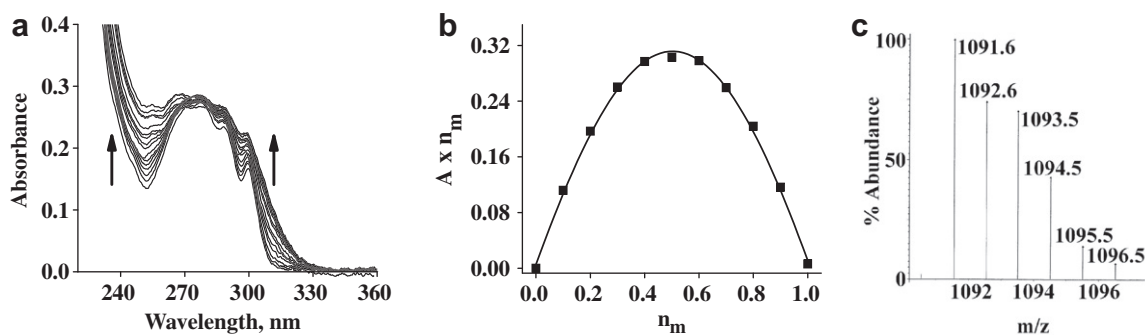


Fig. 4. (a) Absorption spectral traces obtained during the titration of **L** with different mole ratios of Cu^{2+} ; (b) Job's plot to determine the **L** to Cu^{2+} stoichiometry; (c) Expanded ESI-MS spectrum of $[\text{CuL-H}^+]^+$ showing the isotopic pattern.

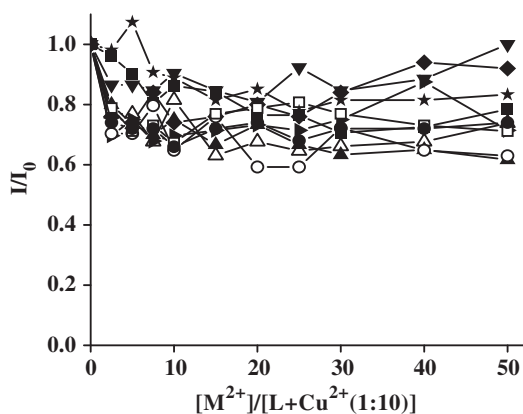


Fig. 5. (a) Plot of fluorescence intensity versus mole ratio of added M^{2+} in a solution contains **L** and Cu^{2+} present as 1:10 ratio. The symbols corresponds to \blacksquare = Mn^{2+} ; \triangle = Fe^{2+} ; \blacktriangle = Co^{2+} ; \blacktriangledown = Ni^{2+} ; \blacktriangleright = Zn^{2+} ; \blacklozenge = Cd^{2+} ; \circ = Hg^{2+} ; \square = Ca^{2+} ; \bullet = Mg^{2+} and \star = Pb^{2+} .

that of the optimized structure of the copper complex revealed only marginal changes in the dihedral angles of the arms (SI 05), while the arms move farther apart to accommodate the Cu^{2+} in the binding core formed by the benzothiazole and amide moieties (Fig. 6b,c). The distances between S1, S2 and O1, O5 were adjusted in such a way that Cu^{2+} can accommodate in the O_2S_2 binding core, where the S1...S2 distance increases from 3.769 to 4.989 Å and the

O1...O5 distance decreases from 6.290 to 3.412 Å on going from simple **L** to its Cu^{2+} complex.

3.6. Anion recognition studies

The Cu^{2+} complex formed with **L** has been further titrated in acetonitrile solution for studying the recognition of anions. These studies were carried out at the same concentration as that of the fluorescence titrations carried out using metal ions. Among the 14 anions, viz., F^- , Cl^- , Br^- , I^- , ClO_4^- , SCN^- , AcO^- , SO_4^{2-} , CO_3^{2-} , NO_3^- , HSO_3^- , HPO_4^{2-} , NO_2^- and N_3^- , studied, only iodide ion exhibit change in the color of the solution from colorless to pale-yellow, where as all other ions showed no change in the color (Fig. 7). Thus the presence of iodide can be visually detected.

Absorption titration carried out between Cu^{2+} and I^- resulted in some spectral changes, such as, the formation of a new band at 362 nm and increase in the absorbance of 244 and 288 nm bands, as can be seen from Fig. 8. No such changes were observed in the absorption spectra in case of other anions (SI 06).

4. Conclusions

In summary, an effective molecular receptor, **L** for the selective recognition of Cu^{2+} followed by iodide, has been synthesized by appropriate derivatization at the lower rim of calix[4]arene and **L** has been characterized. The pre-organized binding core present in **L** is good enough to hold Cu^{2+} even after the addition of excess

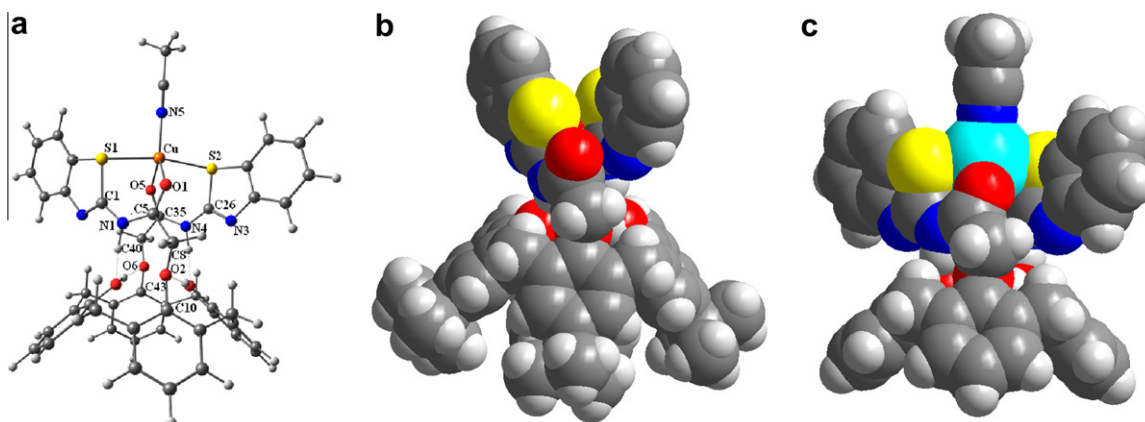


Fig. 6. (a) B3LYP/6-31G* optimized structure of $[\text{CuL}]^{2+}$. The bond distances (Å) and bond angles ($^\circ$) around Cu^{2+} in the coordination sphere are: Cu–N5 = 1.922, Cu–S1 = 2.493, Cu–S2 = 2.522, Cu–O1 = 2.139 and Cu–O5 = 2.095 Å; and S1–Cu–S2 = 168.2, N5–Cu–O1 = 124.1, N5–Cu–O5 = 128.5, O1–Cu–O5 = 107.4, S1–Cu–N5 = 96.2, S1–Cu–O1 = 77.3, S1–Cu–O5 = 95.2, S2–Cu–N5 = 95.5, S2–Cu–O1 = 95.5, S2–Cu–O5 = 77.9 $^\circ$. (b) Space filling model for **L** based on the crystal structure. (c) Space filling model for the optimized structure of the copper complex given under (a).

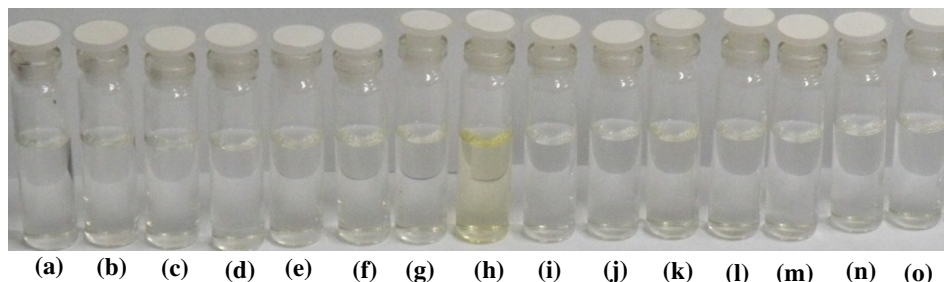


Fig. 7. Color changes observed during the titration of $[\text{CuL}]^{2+}$ by different anions: (a) no anion, (b) SCN^- , (c) HSO_3^- , (d) AcO^- , (e) F^- , (f) Cl^- , (g) Br^- , (h) I^- , (i) ClO_4^- , (j) NO_2^- , (k) N_3^- , (l) NO_3^- , (m) SO_4^{2-} , (n) CO_3^{2-} , (o) HPO_4^{2-} .

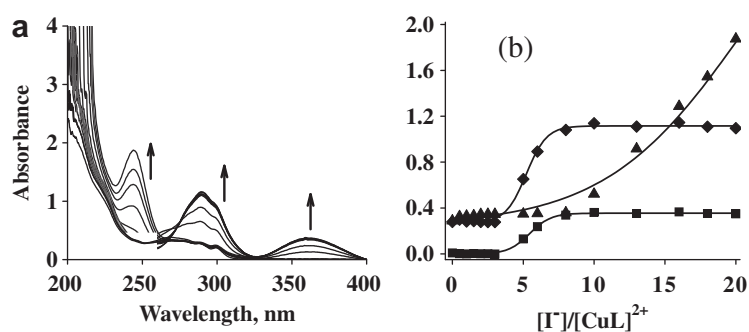


Fig. 8. (a) Spectral traces obtained during the titration of $[\text{CuL}]^{2+}$ (5:1) with increasing mole ratios of I^- , (b) plot of absorbance versus mole ratio of $[\text{I}^-]/[\text{CuL}]^{2+}$ added. Where $\circ = 362$, $\bullet = 288$ and $\star = 244$ nm.

amount of other M^{2+} ions as demonstrated through competitive titrations. Comparison of the fluorescence results of **L** with those of **L**₁ clearly explains the necessity of calix[4]arene platform for selective Cu^{2+} detection. The 1:1 complex formed between Cu^{2+} and **L** was evident from ESI-MS and absorption studies. The ligand, **L** was able to detect Cu^{2+} even at a low concentration of 403 ppb. The ^1H NMR titration revealed the formation of Cu^{2+} complex of **L** by exhibiting broadened signals owing to the presence of paramagnetic Cu^{2+} . The computational calculations carried out in a cascade fashion revealed the formation of a distorted trigonal bipyramidal Cu^{2+} complex, wherein the entry of Cu^{2+} ion seems to be affected by widening the arms so as to take the 'S' centers farther and amide-CO's closer. In the complex, **L** acts as tetradentate ligand providing its ligations through O_2S_2 core, wherein the 5th coordination is filled by the solvent acetonitrile, thus providing structural identity for the species of recognition. The 1:1 complex thus formed exhibits color change in the presence of iodide only among the fourteen anions studied and hence the recognition of iodide selectively.

Acknowledgements

CPR acknowledges the financial support from DST, CSIR and DAE-BRNS. RJ thanks UGC and JPC thanks CSIR for their senior research fellowships respectively. We thank SAIF for ESI-MS and DST's national single crystal XRD facility of IIT Bombay for crystal data.

Appendix A. Supplementary material

Supplementary data associated with this article can be found, in the online version, at doi:10.1016/j.ica.2010.04.005.

References

[1] M.M.O. Pena, J. Lee, D.J. Thiele, *J. Nutr.* 129 (1999) 1251.

- [2] G. Peers, N.M. Price, *Nature* 441 (2006) 341.
 [3] L. Banci, I. Bertini, S. Ciolfi-Baffoni, T. Hadjiloi, M. Martinelli, P. Paluma, *Proc. Nat. Acad. Sci. U.S.A.* 105 (2008) 6803.
 [4] B.G. Malmstrom, J. Leckner, *Curr. Opin. Chem. Biol.* 2 (1998) 286.
 [5] F.D. Rienzo, R.R. Gabdoulline, M.C. Menziani, R.C. Wade, *Protein Sci.* 9 (2000) 1439.
 [6] M.B. Zimmermann, *J. Trace, Elem. Med. Bio.* 22 (2008) 81.
 [7] F. Delange, *Proc. Nutr. Soc.* 59 (2000) 75.
 [8] D.J. Waggoner, T.B. Bartnikas, J.D. Gitlin, *Neurobiol. Dis.* 6 (1999) 221.
 [9] W. Cerpa, L. Varela-Nallar, A.E. Reyes, A.N. Minniti, N.C. Inestros, *Mol. Aspects Med.* 26 (2005) 405.
 [10] N.Q. Liu, Q. Xu, X.L. Hou, P.S. Liu, Z.F. Chai, L. Zhu, Z.Y. Zhao, Z.H. Wang, Y.F. Li, *Brain Res. Bull.* 55 (2001) 309.
 [11] A. Kotwal, R. Priya, I. Qadeer, *Arch. Med. Res.* 38 (2007) 1.
 [12] L. Mandolini, R. Ungaro, Imperial College Press., London, 2000.
 [13] J.S. Kim, D.T. Quang, *Chem. Rev.* 107 (2007) 3780.
 [14] B.S. Creaven, D.F. Donlon, J. McGinley, *Coord. Chem. Rev.* 253 (2009) 893.
 [15] A.B. Othman, J.W. Lee, J.-S. Wu, J.S. Kim, R. Abidi, P. Thury, J.M. Strub, A.V. Dorsselaer, J.J. Vicens, *J. Org. Chem.* 72 (2007) 7634.
 [16] J. Lu, X. Tong, X. He, *J. Electroanal. Chem.* 540 (2003) 111.
 [17] R. Métivier, I. Leray, B. Valeur, *Chem. Commun.* (2003) 996.
 [18] Q.-Y. Chen, C.-F. Chen, *Tetrahedron Lett.* 46 (2005) 165.
 [19] R. Métivier, I. Leray, B. Valeur, *Chem. Eur. J.* 10 (2004) 4480.
 [20] K.-C. Chang, L.-Y. Luo, E.W.-G. Diau, W.-S. Chung, *Tetrahedron Lett.* 49 (2008) 5013.
 [21] G.-Ke. Li, Z.-X. Xu, C.-F. Chen, Z.-T. Huang, *Chem. Commun.* (2008) 1774.
 [22] Z. Liang, Z. Liu, L. Jiang, Y. Gao, *Tetrahedron Lett.* 48 (2007) 1629.
 [23] J.-M. Liu, Q.-Y. Zheng, J.-L. Yang, C.-F. Chen, Z.-T. Huang, *Tetrahedron Lett.* 43 (2002) 9209.
 [24] D.T. Quang, H.S. Jung, J.H. Yoon, S.Y. Lee, J.S. Kim, *Bull. Korean Chem. Soc.* 28 (2007) 682.
 [25] Z. Xu, S. Kim, H.N. Kim, S.J. Han, C. Lee, J.S. Kim, X. Qian, J. Yoon, *Tetrahedron Lett.* 48 (2007) 9151.
 [26] B. Bodenant, T. Weil, M. Businelli-Pourcel, F. Fages, B. Barbe, I. Pianet, M.J. Laguerre, *J. Org. Chem.* 64 (1999) 7034.
 [27] Y.-D. Cao, Q.-Y. Zheng, C.-F. Chen, Z.-T. Huang, *Tetrahedron Lett.* 44 (2003) 4751.
 [28] A. Senthilvelan, I.-T. Ho, K.-C. Chang, G.-H. Lee, Y.-H. Liu, W.-S. Chung, *Chem. Eur. J.* 15 (2009) 6152.
 [29] J. Dessingou, R. Joseph, C.P. Rao, *Tetrahedron Lett.* 46 (2005) 7967.
 [30] R.K. Pathak, Sk.Md. Ibrahim, C.P. Rao, *Tetrahedron Lett.* 50 (2009) 2730.
 [31] R. Joseph, B. Ramanujam, H. Pal, C.P. Rao, *Tetrahedron Lett.* 49 (2008) 6257.
 [32] R. Joseph, B. Ramanujam, A. Acharya, C.P. Rao, *Tetrahedron Lett.* 50 (2009) 2735.
 [33] R. Joseph, B. Ramanujam, A. Acharya, A. Khutia, C.P. Rao, *J. Org. Chem.* 73 (2008) 5745.
 [34] R. Joseph, A. Gupta, A. Ali, C.P. Rao, *Indian J. Chem. A* 46A (2007) 1095.

- [35] P.V. Rao, C.P. Rao, E. Kolehmainen, E.K. Wegelius, K. Rissanen, *Chem. Lett.* (2001) 1176.
- [36] D. Kraf, J.-D. Loon, M. Owens, W. Verboom, W. Vogt, M.A. McKervey, V. Boihmer, D.N. Reinhoudt, *Tetrahedron Lett.* 31 (1990) 4941.
- [37] E.M. Collins, M.A. McKervey, E. Madigan, M.B. Moran, M. Owens, G. Ferguson, S.J. Harris, *J. Chem. Soc., Perkin Trans. 1* (1991) 3137.
- [38] V. Bohmer, G. Ferguson, J.F. Gallagher, A.J. Lough, M.A. McKervey, E. adigan, M.B. Moran, J. Phillips, G. Williams, *J. Chem. Soc., Perkin Trans. 1* (1993) 1521.
- [39] M.J. Frisch, G.W. Trucks, H.B. Schlegel, G.E. Scuseria, M.A. Robb, J.R. Cheeseman, J.A. Montgomery Jr, T. Vreven, K.N. Kudin, J.C. Burant, J.M. Millam, S.S. Iyengar, J. Tomasi, V. Barone, B. Mennucci, M. Cossi, G. Scalmani, N. Rega, G.A. Petersson, H. Nakatsuji, M. Hada, M. Ehara, K. Toyota, R. Fukuda, J. Hasegawa, M. Ishida, T. Nakajima, Y. Honda, O. Kitao, H. Nakai, M. Klene, X. Li, J.E. Knox, H.P. Hratchian, J.B. Cross, V. Bakken, C. Adamo, J. Jaramillo, R. Gomperts, R.E. Stratmann, O. Yazyev, A.J. Austin, R. Cammi, C. Pomelli, J.W. Ochterski, P.Y. Ayala, K. Morokuma, G.A. Voth, P. Salvador, J.J. Dannenberg, V.G. Zakrzewski, S. Dapprich, A.D. Daniels, M.C. Strain, O. Farkas, D.K. Malick, A.D. Rabuck, K. Raghavachari, J.B. Foresman, J.V. Ortiz, Q. Cui, A.G. Baboul, S. Clifford, J. Cioslowski, B.B. Stefanov, G. Liu, A. Liashenko, P. Piskorz, I. Komaromi, R.L. Martin, D.J. Fox, T. Keith, M.A. Al-Laham, C.Y. Peng, A. Nanayakkara, M. Challacombe, P.M.W. Gill, B. Johnson, W. Chen, M.W. Wong, C. Gonzalez, J.A. Pople, *GAUSSIAN 03*, Revision C.02, Gaussian, Inc., Wallingford CT, 2004.